Available online at www.sciencedirect.com
SCIENCE DIRECT®
International Journal of Thermal Sciences 44 (2005) 342–348
International Journal of Thermal Sciences
www.elsevier.com/locate/ijts

Constructal tree-shaped fins

Majed A. Almogbel

Refrigeration and Air-Conditioning Division, Riyadh College of Technology, PO Box 86119, Riyadh 11622, Saudi Arabia

Received 3 September 2004; received in revised form 23 November 2004; accepted 30 November 2004

Abstract

A tree-like fin is investigated and optimized by the constructal optimization method. The tree shape is not mimicked. Rather, the T-shaped fin—which was optimized in a previous paper—is enhanced geometrically. This fin is allowed to grow new branches to allow more of the fin-material to get to the surface area and transfer heat directly to the reservoir. For that, the new fin is adding more branches in each major step of the optimization process until an optimum shape—that delivers the maximum base heat—is found. Fin material (volume fraction) and fin allocated volume (frontal area) are constrained. In this paper the tree-shaped fin is kept uniform as in uniform thicknesses of the stem and the branches, and an equal length and equal thicknesses of all branches. The thermal performance of the optimized tree-shaped fin is found to be much better than the performance of the longitudinal fin and the optimized T-shaped fins, and it has a compact size.

Keywords: Tree-shaped fins; T-shaped fins; Extended surfaces; Constructal optimization; Thermal performance

1. Introduction

Fins have long been recognized as effective means to augment heat transfer. The literature on this subject is sizeable. In recent paper [1], Bejan and Almogbel have contributed to this effort by the utilization of constructal optimization method. The new aspect that is contributed by the constructal method is the complete geometric optimization of the fin when the total inhabited volume is fixed. In order to illustrate this aspect in the most transparent terms, the authors have applied the constructal optimization method to some of the simplest assembly types that have been recognized in practice. Three assembly configurations have been optimized. The simplest was the T-shaped fin, for which was shown that the constructal optimization can lead to substantial increase in global conductance relative to longitudinal fin and to previously optimized (by different method) T-shaped fin designs that fill the same volume and use the same amount of fin material (e.g., Table 1).

Table 1
Numerical examples of optimized fins ($\phi_1 = 0.086$, $a = 0.185$)

Fin design	$\tilde{q}_B$	Aspect ratio
Optimized longitudinal fin	0.031	2.95*
T-shaped fin optimized by Kraus [5]	0.040	0.4829
Constructal optimized T-shaped fin [1]	0.0516	0.141
Double-constrained tree-shaped fin	0.0712	1

* Using the same frontal area of other designs.

Another useful result that was revealed for the constructal optimized T-shaped fin was that certain architectural features are relatively "robust", i.e., insensitive to changes in design parameters. The feature of robustness was important for the constructal T-shaped fin because the aspect ratio of its optimized shape was found to be geometrically impractical, especially for compact applications as in heat sinks of notebook computers and miniature electronic devices.

In order to enhance the thermal performance of the optimized T-shaped fin, and to overcome its geometrical impracticality, it must be allowed to evolve. In this paper, the T-shaped fin is allowed to grow new branches to allow more of the fin-material to get to the surface area to transfer heat directly to the reservoir. Starting from the T-shape, the new fin adds more branches in each major step of the optimiza-

E-mail address: majedalmogbel@yahoo.com (M.A. Almogbel).

1290-0729/$ – see front matter
doi:10.1016/j.ijthermalsci.2004.11.002

Nomenclature

A	frontal allocated area of the fin	m^2
A_f	fin material cross-sectional area	m^2
h	heat transfer coefficient	$W{\cdot}m^{-2}{\cdot}K^{-1}$
i_{max}	maximum number of branch pairs	
k	thermal conductivity	$W{\cdot}m^{-1}K^{-1}$
L_i	length of stem portion i	m
L_{bi}	length of branch i	m
q_B	overall heat conductance	W
q_{bi}	branch i base heat transfer rate	W
t_i	thickness of stem portion i	m
t_{bi}	thickness of branch i	m
T_i	temperature at junction i	K
T_x	temperature at stem length x	K

Greek symbols

ϕ	volume fraction of fin material
θ	dimensionless temperature

Subscripts

opt	optimum
i	stem or branch pair number
b	branch
m	maximized once
mm	maximized twice

Superscript

$\sim$	dimensionless notation

tion process until an optimum shape, that delivers the maximum base heat- is found. Fin material (volume fraction) and fin allocated volume (frontal area) are constrained. Stem lengths ratios, branches lengths ratios, stem thicknesses ratios, and branches thicknesses ratios are all fixed. The simplifications of the constructal T-shaped fin [1] are adopted here too; a unidirectional conduction model is assumed and a uniform heat transfer coefficient for the flow over the fin surface.

2. Unidirectional conduction model

Consider the tree-shaped assembly of fins sketched in Fig. 1, multiple "elemental" fins (branches) of thicknesses t_{bi} and lengths L_{bi} (bi denotes branch pair number i) serve as tributaries to a stem portions of thicknesses t_i and lengths L_i (i denotes the stem portion that branch pair number bi is connected to, at top). By having only one level of branching the shape in Fig. 1 represents a first construct of the tree-shaped fin. The thicknesses and lengths of all branches are made equal, so are the thicknesses and lengths of all stem portions. The configuration is two-dimensional, with the third dimension (W) sufficiently long in comparison with $L_{i_{max}}$ and $L_{bi_{max}}$. The heat transfer coefficient (h) is uniform overall the exposed surfaces. Specified are the temperatures of the root (T_B) and the fluid (T_∞). The temperatures at the junctions (T_i) are unknowns, and vary with the geometry of the assembly.

The objective of the following analysis is to determine the optimal geometry that is characterized by the maximum global thermal conductance $q_B/(T_B - T_\infty)$, where q_B is the heat current through the base of the stem. The optimal geometry is represented by the overall aspect ratio of the tree-shaped fin ($L_{i_{max}}/2L_{bi_{max}}$) or slenderness, the individual branches-to-stem aspect ratio (t_{bi}/t_i), and the number of branch pairs (i_{max}). The optimization is subjected to two

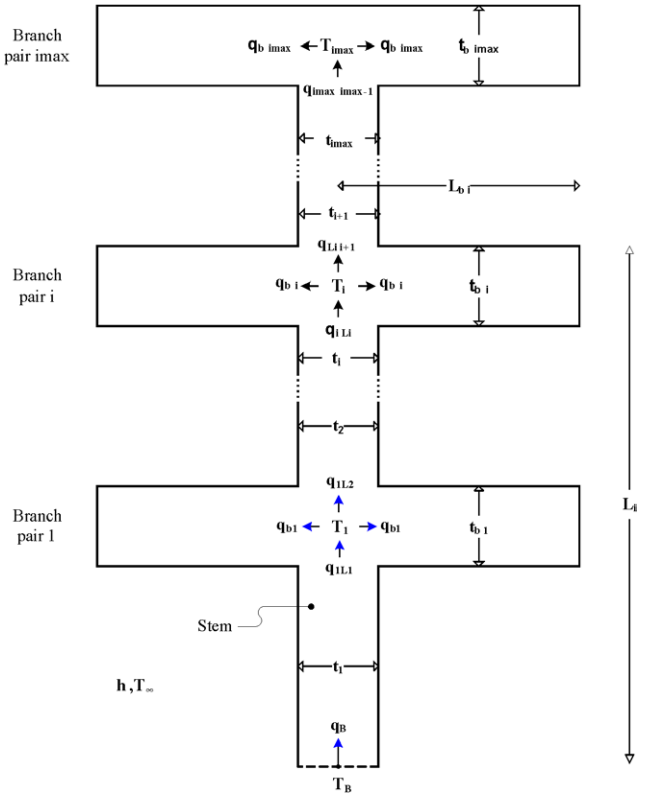

Fig. 1. A tree-shaped fin.

constraints, namely, the total volume (i.e., frontal allocated area) constraint,

$$A = 2L_{i_{max}}L_{bi_{max}} \quad \text{(constant)} \tag{1}$$

and the fin-material volume constraint,

$$A_f = \sum_{1}^{i_{max}} (2L_{bi}t_{bi} + t_i L_i) \quad \text{(constant)} \tag{2}$$

The latter can be expressed as the fin volume fraction $\phi = A_f/A$, which is a constant considerably smaller than 1.

The analysis that delivers the global conductance as a function of the assembly geometry consists of accounting for conduction along the stem and the branches, and invoking the continuity of temperature and heat currents at the junctions. The assumptions of a unidirectional conduction model [2] are used for the stem and the branches. The validity of this model is tested later in Eqs. (13), (14).

The solution for a fin with non-negligible heat transfer through the tip [2] is applied for the branches,

$$\frac{q_{\mathrm{b}i}}{kW(T_i-T_\infty)} = a\tilde{t}_{\mathrm{b}i}^{1/2}\frac{2\sinh(a\widetilde{L}_{\mathrm{b}i}\tilde{t}_{\mathrm{b}i}^{-1/2})+a\tilde{t}_{\mathrm{b}i}^{1/2}\cosh(a\widetilde{L}_{\mathrm{b}i}\tilde{t}_{\mathrm{b}i}^{-1/2})}{2\cosh(a\widetilde{L}_{\mathrm{b}i}\tilde{t}_{\mathrm{b}i}^{-1/2})+a\tilde{t}_{\mathrm{b}i}^{1/2}\sinh(a\widetilde{L}_{\mathrm{b}i}\tilde{t}_{\mathrm{b}i}^{-1/2})} \quad (3)$$

where

$$\left(\widetilde{L}_{\mathrm{b}i},\tilde{t}_{\mathrm{b}i}\right)=\frac{(L_{\mathrm{b}i},t_{\mathrm{b}i})}{A^{1/2}},\qquad a=\left(\frac{2hA^{1/2}}{k}\right)^{1/2} \quad (4,5)$$

Eq. (3) shows the emergence of the dimensionless parameters $(a,\widetilde{L}_{\mathrm{b}i},\tilde{t}_{\mathrm{b}i})$ which influence the dimensionless branches conductance $\tilde{q}_{\mathrm{b}i}=q_{\mathrm{b}i}/[kW(T_i-T_\infty)]$. Note the use of $A^{1/2}$ as length scale in the nondimensionalization of the linear dimensions.

The temperature distribution along the stem portion i, T_x, from the root of the stem ($x=L_{i-1}$) to the junction at the top ($x=L_i$), is

$$T_x-T_\infty=C1\cdot\sinh(m_ix)+C2\cdot\cosh(m_ix) \quad (6)$$

where

$$C1=\frac{(T_{i-1}-T_\infty)}{\sinh(m_iL_{i-1})}\big[\sinh(m_iL_{i-1})\cosh(m_iL_i)-\theta_{i,i-1}\sinh(m_iL_{i-1})\cosh(m_iL_{i-1})-2\sinh(m_iL_i)\cosh(m_iL_{i-1})\big]\times\big[\sinh(m_iL_{i-1})\cosh(m_iL_i)-\sinh(m_iL_i)\cosh(m_iL_{i-1})\big]^{-1}$$

$$C2=(T_{i-1}-T_\infty)\big[\theta_{i,i-1}\sinh(m_iL_{i-1})-\sinh(m_iL_i)\big]\times\big[\sinh(m_iL_{i-1})\cosh(m_iL_i)-\sinh(m_iL_i)\cosh(m_iL_{i-1})\big]^{-1}$$

The fin parameter $m_i=(2h/kt_i)^{1/2}$ can be expressed as $m_iL_i=a\widetilde{L}_i\tilde{t}_i^{-1/2}$. Next, T_x is substituted in the equation for the continuity of heat current at the junctions, $q_i=q_{i+1}+2q_{\mathrm{b}i}$

$$-kt_iW\left(\frac{\partial T}{\partial x}\right)_{x=L_i}=-kt_{i+1}W\left(\frac{\partial T}{\partial x}\right)_{x=L_i}+2q_{\mathrm{b}i} \quad (7)$$

which can be arranged in a dimensionless form, and solved to establish the dimensionless junction temperature, $\theta_{i,i-1}=(T_i-T_\infty)/(T_{i-1}-T_\infty)$, as a function of the dimensionless parameters of the fin assembly (a, $\widetilde{L}_i$, $\tilde{t}_i$, $\widetilde{L}_{i-1}$, $\widetilde{L}_{i+1}$, $\tilde{t}_{i+1}$, $\widetilde{L}_{\mathrm{b}i}$, $\tilde{t}_{\mathrm{b}i}$, $\theta_{i+1,i}$),

$$\theta_{i,i-1}=\frac{\eta}{\alpha+\beta-\gamma+\zeta} \quad (8)$$

where

$$\eta=\big[\sinh(a\widetilde{L}_i\tilde{t}_i^{-1/2})^2-\cosh(a\widetilde{L}_i\tilde{t}_i^{-1/2})^2\big]\times\big[\sinh(a\widetilde{L}_{i-1}\tilde{t}_i^{-1/2})\cosh(a\widetilde{L}_i\tilde{t}_i^{-1/2})-\sinh(a\widetilde{L}_i\tilde{t}_i^{-1/2})\cosh(a\widetilde{L}_{i-1}\tilde{t}_i^{-1/2})\big]^{-1}$$

$$\alpha=\big[\sinh(a\widetilde{L}_i\tilde{t}_i^{-1/2})\sinh(a\widetilde{L}_{i-1}\tilde{t}_i^{-1/2})-\cosh(a\widetilde{L}_i\tilde{t}_i^{-1/2})\cosh(a\widetilde{L}_{i-1}\tilde{t}_i^{-1/2})\big]\times\big[\sinh(a\widetilde{L}_{i-1}\tilde{t}_i^{-1/2})\cosh(a\widetilde{L}_i\tilde{t}_i^{-1/2})-\sinh(a\widetilde{L}_i\tilde{t}_i^{-1/2})\cosh(a\widetilde{L}_{i-1}\tilde{t}_i^{-1/2})\big]^{-1}$$

$$\beta=\left(\frac{t_{i+1}}{t_i}\right)^{1/2}\big[\sinh(a\widetilde{L}_{i+1}\tilde{t}_{i+1}^{-1/2})\sinh(a\widetilde{L}_i\tilde{t}_{i+1}^{-1/2})-\cosh(a\widetilde{L}_{i+1}\tilde{t}_{i+1}^{-1/2})\cosh(a\widetilde{L}_i\tilde{t}_{i+1}^{-1/2})\big]\times\big[\sinh(a\widetilde{L}_i\tilde{t}_{i+1}^{-1/2})\cosh(a\widetilde{L}_{i+1}\tilde{t}_{i+1}^{-1/2})-\sinh(a\widetilde{L}_{i+1}\tilde{t}_{i+1}^{-1/2})\cosh(a\widetilde{L}_i\tilde{t}_{i+1}^{-1/2})\big]^{-1}$$

$$\gamma=\left(\frac{t_{i+1}}{t_i}\right)^{1/2}\theta_{i+1,i}\big[\sinh(a\widetilde{L}_i\tilde{t}_{i+1}^{-1/2})^2-\cosh(a\widetilde{L}_i\tilde{t}_{i+1}^{-1/2})^2\big]\times\big[\sinh(a\widetilde{L}_i\tilde{t}_{i+1}^{-1/2})\cosh(a\widetilde{L}_{i+1}\tilde{t}_{i+1}^{-1/2})-\sinh(a\widetilde{L}_{i+1}\tilde{t}_{i+1}^{-1/2})\cosh(a\widetilde{L}_i\tilde{t}_{i+1}^{-1/2})\big]^{-1}$$

$$\zeta=2\left(\frac{t_{\mathrm{b}i}}{t_i}\right)^{1/2}\frac{2\sinh(a\widetilde{L}_{\mathrm{b}i}\tilde{t}_{\mathrm{b}i}^{-1/2})+a\tilde{t}_{\mathrm{b}i}^{1/2}\cosh(a\widetilde{L}_{\mathrm{b}i}\tilde{t}_{\mathrm{b}i}^{-1/2})}{2\cosh(a\widetilde{L}_{\mathrm{b}i}\tilde{t}_{\mathrm{b}i}^{-1/2})+a\tilde{t}_{\mathrm{b}i}^{1/2}\sinh(a\widetilde{L}_{\mathrm{b}i}\tilde{t}_{\mathrm{b}i}^{-1/2})}$$

Similar analysis of the top most junction ($x=L_{i_{\max}}$) of the tree-shaped fin reveals its dimensionless junction temperature, $\theta_{i_{\max},i_{\max}-1}$, which is a function of only five parameters (a, $\widetilde{L}_{i_{\max}}$, $\tilde{t}_{i_{\max}}$, $\widetilde{L}_{i_{\max}-1}$, $\widetilde{L}_{\mathrm{b}i_{\max}}$, $\tilde{t}_{\mathrm{b}i_{\max}}$),

$$\theta_{i_{\max},i_{\max}-1}=\frac{\varphi}{\lambda+\psi} \quad (9)$$

where

$$\varphi=\big[\sinh(a\widetilde{L}_{i_{\max}}\tilde{t}_{i_{\max}}^{-1/2})^2-\cosh(a\widetilde{L}_{i_{\max}}\tilde{t}_{i_{\max}}^{-1/2})^2\big]\times\big[\sinh(a\widetilde{L}_{i_{\max}-1}\tilde{t}_{i_{\max}}^{-1/2})\cosh(a\widetilde{L}_{i_{\max}}\tilde{t}_{i_{\max}}^{-1/2})-\sinh(a\widetilde{L}_{i_{\max}}\tilde{t}_{i_{\max}}^{-1/2})\cosh(a\widetilde{L}_{i_{\max}-1}\tilde{t}_{i_{\max}}^{-1/2})\big]^{-1}$$

$$\lambda=\big[\sinh(a\widetilde{L}_{i_{\max}}\tilde{t}_{i_{\max}}^{-1/2})\sinh(a\widetilde{L}_{i_{\max}-1}\tilde{t}_{i_{\max}}^{-1/2})-\cosh(a\widetilde{L}_{i_{\max}}\tilde{t}_{i_{\max}}^{-1/2})\cosh(a\widetilde{L}_{i_{\max}-1}\tilde{t}_{i_{\max}}^{-1/2})\big]\times\big[\sinh(a\widetilde{L}_{i_{\max}-1}\tilde{t}_{i_{\max}}^{-1/2})\cosh(a\widetilde{L}_{i_{\max}}\tilde{t}_{i_{\max}}^{-1/2})-\sinh(a\widetilde{L}_{i_{\max}}\tilde{t}_{i_{\max}}^{-1/2})\cosh(a\widetilde{L}_{i_{\max}-1}\tilde{t}_{i_{\max}}^{-1/2})\big]^{-1}$$

$$\psi=2\left(\frac{t_{\mathrm{b}i_{\max}}}{t_{i_{\max}}}\right)^{1/2}\times\frac{2\sinh(a\widetilde{L}_{\mathrm{b}i_{\max}}\tilde{t}_{\mathrm{b}i_{\max}}^{-1/2})+a\tilde{t}_{\mathrm{b}i_{\max}}^{1/2}\cosh(a\widetilde{L}_{\mathrm{b}i_{\max}}\tilde{t}_{\mathrm{b}i_{\max}}^{-1/2})}{2\cosh(a\widetilde{L}_{\mathrm{b}i_{\max}}\tilde{t}_{\mathrm{b}i_{\max}}^{-1/2})+a\tilde{t}_{\mathrm{b}i}^{1/2}\sinh(a\widetilde{L}_{\mathrm{b}i_{\max}}\tilde{t}_{\mathrm{b}i_{\max}}^{-1/2})}$$

Finally, the global thermal conductance is obtained by applying the continuity equation for the heat current through

the root, $q_B = q_{i=1}$ $(x = 0)$. The result can be expressed as a dimensionless global conductance of the tree-shaped fin,

$$\tilde{q}_B = \frac{q_B}{kW(T_B - T_\infty)} = a\tilde{t}_1^{1/2}\frac{\cosh(a\tilde{L}_1\tilde{t}_1^{-1/2}) - \theta_{1,B}}{\sinh(a\tilde{L}_1\tilde{t}_1^{-1/2})} \quad (10)$$

for which $\theta_{1,B} = (T_1 - T_\infty)/(T_B - T_\infty)$. Following the concatenation of Eqs. (9), (8), then (10), provides the global conductance of the tree-shaped fin $\tilde{q}_B$ as a function of a, $\tilde{L}_i$, $\tilde{t}_i$, $\tilde{L}_{bi}$ and $\tilde{t}_{bi}$: only three of these groups of parameters are free to vary, because of the volume and fin material constraints (Eqs. (1) and (2)), which now read

$$2\tilde{L}_{i_{max}}\tilde{L}_{bi_{max}} = 1 \quad (11)$$

$$\phi = \sum_1^{i_{max}} \left(2\tilde{L}_{bi}\tilde{t}_{bi} + \tilde{t}_i\tilde{L}_i\right) \quad (12)$$

In the optimization code, the number of branches levels (number of pairs of branches, i_{max}), the slenderness (overall aspect ratio) of the tree-shaped fin, and the branches-to-stem thickness ratio are used as degrees of freedom. Discrete values are assigned for other parameters, where the geometric parameters were fixed as equal branches lengths, equal branches thicknesses, and equal stem portions thicknesses. The fin parameter (a) is fixed at the value 0.185, and the fin volume fraction, ϕ, is fixed at 0.086.

Note that when the optimum ratio $(t_{bi}/t_i)_{opt}$ is known, the individual thicknesses $(\tilde{t}_{bi,opt}, \tilde{t}_{i,opt})$ can be calculated easily from the material constraint (Eq. (12)). Similarly, when the optimum overall aspect ratio of the fin $(L_{i_{max}}/2L_{bi})_{opt}$ is known, the individual lengths $(\tilde{L}_{i,opt}, \tilde{L}_{bi,opt})$ follow immediately from the volume constraint (Eq. (11)).

3. Optimal tree-shaped geometry

Results for the optimal geometry of the tree-shaped fin can be generated by using the procedure sequence of Figs. 2–5. The adopted procedure is a full optimization procedure that scans all—and more than—practical geometries of the fin. The optimization sequence was to fix all variables then to search for the optimum value of branches-to-stem thickness ratio. Finding an optimum branches-to-stem thickness ratio for various values of the overall aspect ratio of the fin is the second step in the sequence and leads to an optimum slenderness. Varying the number of pairs of branches, i_{max}, while repeating the previous two steps for every value of i_{max} comprises the final step of the optimization sequence in the effort to find an optimum number of branches of the tree-shaped fin.

Fig. 2 shows that $\tilde{q}_B$ can be maximized with respect to branch-to-stem thickness ratio t_{bi}/t_i, i.e., with respect to the internal shape of the fin assembly. The peak value of this curve is the maximized overall heat conductance, $\tilde{q}_{B,m}$, that corresponds to the optimum branch-to-stem thickness ratio, $(t_{bi}/t_i)_{opt}$, in a tree-shaped fin that has an overall aspect ratio of 0.25 and six branches. In Fig. 3, the aspect ratio of the fin assembly is varied and an optimum branch-to-stem thickness ratio with a corresponding maximized overall heat conductance is found for each discrete value of the aspect ratio. Here, the maximized overall conductance $\tilde{q}_{B,m}$ is maximized again with respect to the slenderness of the tree-shaped fin, $(L_{i_{max}}/2L_{bi})$. The effort of Fig. 3 is summarized in Fig. 4 as one curve that connects $\tilde{q}_{B,m}$ values that corresponds to different aspect ratios. The peak of Fig. 4 is the twice-maximized overall heat conductance of the tree-shaped fin. The end-result of this double maximization is the twice-maximized overall heat conductance $\tilde{q}_{1,mm}$ shown in Fig. 5, where the double maximization procedure was repeated for a wide range of the number of pairs of branches of the tree-shaped fin, i_{max}.

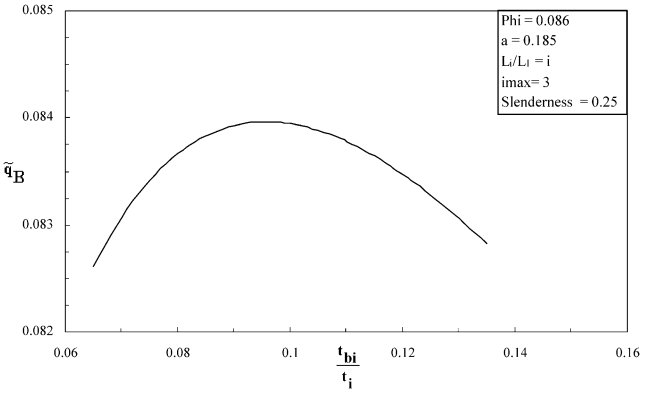

Fig. 2. Optimizing the branches-to-stem thickness ratio for a fixed i_{max} and aspect ratio.

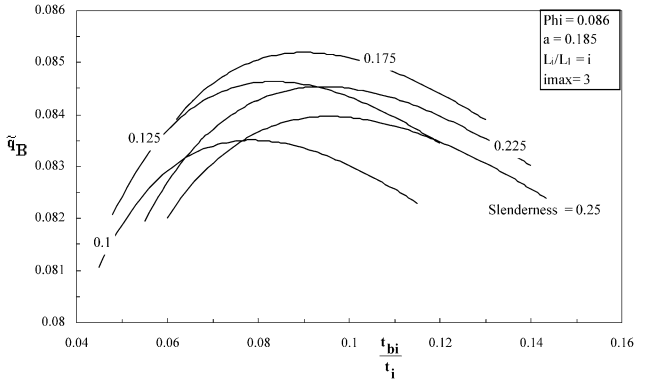

Fig. 3. Optimizing the branches-to-stem thickness ratio for different values of the aspect ratio and a fixed i_{max}.

In this extensive numerical optimization work it is necessary to keep in mind the range of validity of the unidirectional conduction model on which the analysis is based. The model is valid when the following Biot number criterion is satisfied [3]:

$$\left(\frac{ht}{k}\right)^{1/2} \ll 1 \quad (13)$$

According to this criterion, the dimensionless thicknesses $(\tilde{t}_i, \tilde{t}_{bi})$ must be small enough so that

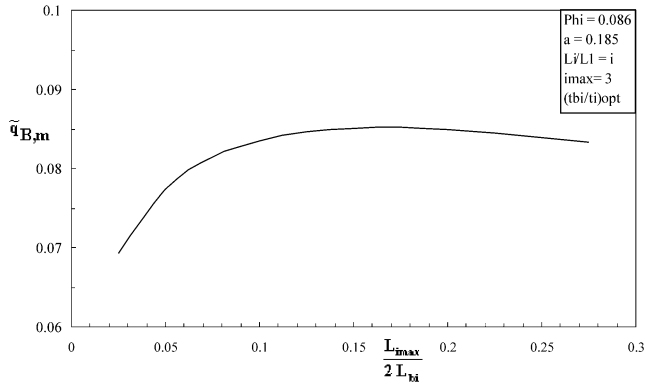

Fig. 4. The once maximized overall conductance is maximized again with respect to the overall aspect ratio.

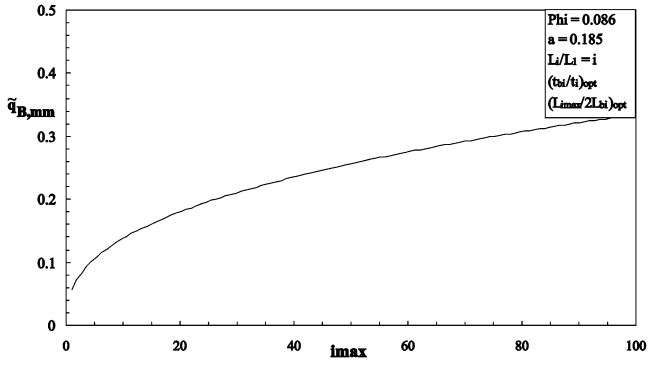

Fig. 5. The improvement of the twice-optimized overall heat conductance with increasing number of pairs of branches, $i_{\max}$.

$$a\left(\frac{\tilde{t}_i}{2}\right)^{1/2} < \varepsilon \quad \text{and} \quad a\left(\frac{\tilde{t}_{bi}}{2}\right)^{1/2} < \varepsilon \tag{14}$$

where ε is a number smaller than 1. The numerical results described in this study satisfy the condition (14) with $\varepsilon = 0.1$, where Biot numbers for all stem portion and all branches were in the range of 0.005–0.037.

Fig. 5 shows that the overall conductance of the tree-shaped fin increases as the number of pairs of branches, $i_{\max}$, increases. This means that the performance of the tree-shaped fin is ever increasing with more complexity; the engineering practicality is the limit. Having no overall optimal tree-shaped geometry is conceivable; because more branches means more fin material is getting to the surface of the fin and transferring heat directly to the reservoir. Note that the individual configurations of Fig. 5 are all optimized both internally and externally for every value of $i_{\max}$. Hence, the geometry of the stem and the branches are mutually enhanced so that only heat-delivery material is optimally put on the surface to increase the overall heat transfer from the fin. This is an important result especially for the constructal optimization method, because it means that—during optimization—constructal optimization method enables the designer to avoid heat delivery choking in extended surface arrays. Heat delivery choking is the phenomenon that Kraus et al. [4] has faced during optimization of extended surface arrays where the stem at some chosen dimensions cannot transfer less heat than the branches can dissipate. In constructal optimization method of fin arrays this limitation does not exist because the whole geometry of the fin assembly is optimized together. Another important characteristic of the tree-shaped fin revealed in Fig. 5 is that the slope of the tangent of $i_{\max} - q_{B,mm}$ curve decreases as $i_{\max}$ increases, i.e., the curve tends to get horizontal as more branches are developed for the fin. This result is particularly important because it means that the tree-shaped fin is going to reach a point of diminishing returns, i.e., a point where more engineering complexity is not justified by the little gain in overall heat conductance.

4. Constrained tree-shaped geometry

An important problem in fin assemblies design is the maximization of global thermal conductance in situations where the shape or the given volume is fixed. For example, available space is a major constraint during design of notebook computers or miniature electronic devices. Manufacturing limits pose other constraints. For the tree-shaped fin, it is now obvious that for every specified number of branches there is an optimum geometry of the fin that would deliver the maximum base heat. But what if the aspect ratio of the fin (space constraint) or the branches-to-stem thickness ratio (manufacturing constraint) is to be specified?

To answer such questions, first the tree-shaped fin was constrained to a specific branches-to-stem thickness ratio ($t_{bi}/t_i = 0.25$), then the optimization of the tree-shaped fin was carried out in a similar manner as in the previous section. Fig. 6 is the result of this optimization. Interestingly it shows that if the branches-to-stem thickness ratio is constrained an optimum number of branch pairs would be found. The optimum number of branch pairs when $t_{bi}/t_i = 0.25$ is 6 (i.e., 12 branches) with a corresponding twice-maximized conductance of 0.0802. For an unconstrained tree-shaped fin with 6 pairs of branches the maximized global conductance is 0.116 (44% better than the constrained fin) but with a branches-to thickness ratio as low as 0.045. The tree-shaped fin was then constrained to specific aspect ratios (Fig. 7). No optimum number of branch pairs was found this case.

A third possibility is to apply two constrains to the tree-shaped fin and search for an optimum configuration. Figs. 2 and 3 already show the behavior of a tree-shaped fin constrained to both specific number of branches and specific slenderness. For every constrained configuration as such, there is an optimum geometry that delivers a maximized heat rate. Similarly, Fig. 6 is the result of a first stage of optimization that had constrained geometries relative to both the number of branch pairs and the stem-to-thickness ratio. Although it is not shown, for every constrained configuration in that stage there was an optimum geometry—with an optimum slenderness—that delivers a maximum heat rate; otherwise no optimum would show up in Fig. 6. The new dou-

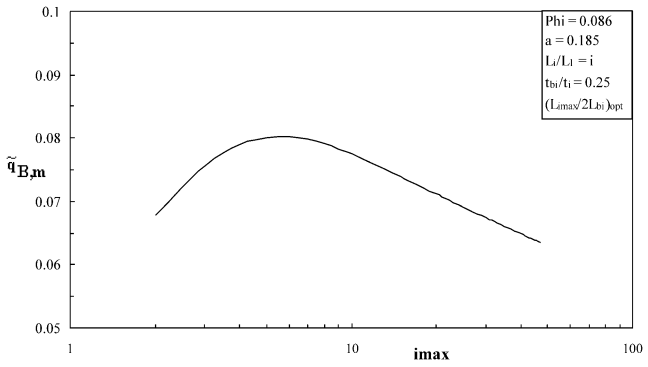

Fig. 6. The optimization of a constrained tree-shaped fin, $t_{bi}/t_i = 0.25$.

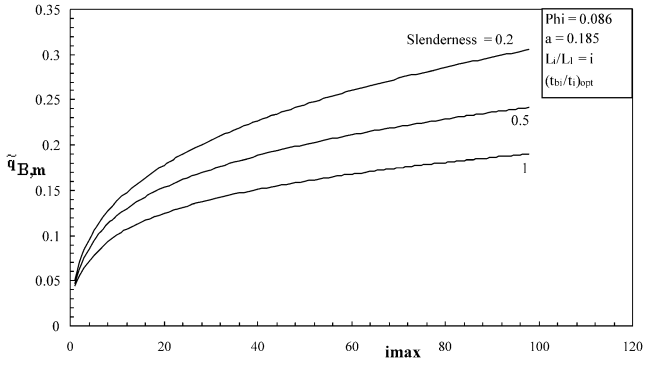

Fig. 7. The optimization of a constrained tree-shaped fin, aspect ratio = 0.2, 0.5, and 1.

ble constrained situation to explore is to constrain the tree-shaped fin to both specific slenderness and specific stem-to-thickness ratio; would there be an optimum configuration with an optimum number of branch pairs that delivers a maximum heat for this situation? Fig. 8 answers this question by showing an optimum configuration with $i_{\max,\mathrm{opt}} = 12$.

It is now proven that more freedom to the tree-shaped fin is a synonym to better performance, but not to practical or preferred shape. This finding is common in other works in the area of constructal design (example, Ref. [9]). The good news in all of this is that in all cases; free, constrained, or double constrained, the tree-shaped has shown a substantial increase in performance than optimized longitudinal fin and optimized T-shaped fins. This means that even if one would sacrifice a little performance to have a preferred-shape constrained tree-shaped fin, it still would be better performer than other fin designs. To show this, a numerical example of the optimized tree-shaped fin constrained to a specific slenderness (aspect ratio = 1) and to a specific branches-to-stem thickness ratio ($t_{bi}/t_i = 0.25$) is presented in Table 1. This example corresponds to a case optimized in an earlier study by Kraus [5], who used $k = 200\ \mathrm{W{\cdot}m^{-1}{\cdot}K^{-1}}$, $h = 60\ \mathrm{W{\cdot}m^{-2}{\cdot}K^{-1}}$ and fin lengths and thicknesses that required a total frontal area $A = 32.4\ \mathrm{cm}^2$ and solid volume fraction $\phi_1 = 0.086$. In this case $a = 0.185$, cf. Eq. (5). The four designs of Table 1 satisfy the assumed unidirectional conduction model.

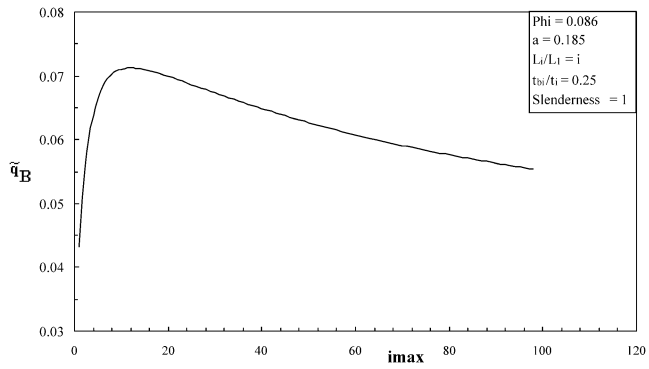

Fig. 8. The optimization of a double-constrained tree-shaped fin, aspect ratio = 1, and $t_{bi}/t_i = 0.25$.

Table 1 shows that the chosen tree-shaped fin surpassed its closest competitor by about 40% improvement in performance. Keep in mind that this chosen tree-shaped fin is double constrained. In fact, it was chosen this way and given an aspect ratio = 1, and a specific stem-to-thickness ratio, $t_{bi}/t_i = 0.25$, only to keep it far from the optimum free tree-shaped fin for the comparison to be unbiased. For example, an unconstrained tree-shaped fin with 12 pairs of branches (as in the double-constrained tree-shaped fin of Table 1) has an overall thermal conductance of 0.15, i.e., has about 200% improvement over the constructal optimized T-shaped fin. Although better performer, this free tree-shaped fin has an optimum aspect ratio of 0.129 (too slim) and an optimum branch-to-stem thickness ratio of 0.02 (very thin), which makes the chosen double-constrained tree-shaped fin a better choice with a lower performance. The summarized result of these comparisons is that tree-shaped fins show a promising fin design with a substantial increase in performance and a very good range of design freedom (robustness) to accommodate a various heat transfer needs.

5. Conclusions

The analysis and optimization work presented in this paper showed that the global thermal conductance of tree-shaped fin could be maximized by geometric optimization subject to total volume and fin material constraints. The optimization and the constraints deliver every geometric feature of the fin. Noteworthy is the emergence of an optimal internal shape characteristic (e.g., the branches-to-stem thickness ratio, Fig. 2) and an optimal external shape for the assembly (e.g., the overall aspect ratio, Fig. 4). The performance of the twice-optimized tree-shaped fin increases as the number of pairs of branches increases. The constructal optimization of tree-shaped fin leads to substantial increases in global conductance relative to current optimal designs that fill the same volume and use the same amount of fin material (e.g., Table 1). Although, the improvement in performance of the tree-shaped fin with respect to con-

tinuing branching reaches a point of dimensioning returns, where more geometric complexity is not justified by the corresponding little gain of performance. An important characteristic of the constructal optimization method was revealed in this paper, that is: the constructal optimization method avoids heat delivery choking in extended surface arrays [4].

The ever-increasing performance of the tree-shaped fin with continuing branching is also related to the idealizations that have been adopted. An important idealization is the assumption that the heat transfer coefficient is independent of the free flow area shape (unidirectional fin model). Future studies may address the effect of relaxing this assumption on tree-shaped architecture. An example of how one may proceed is given in Refs. [6,7], and in the summarizing book of the area of constructal design "Shape and Structure from Engineering to Nature " [8], where the heat transfer coefficient was linked to (i.e., derived from) the optimal spacing between adjacent parallel plates.

References

[1] A. Bejan, M. Almogbel, Constructal T-shaped fins, Internat. J. Heat Mass Transfer 43 (2000) 2110–2115.
[2] A. Aziz, Optimum dimensions of extended surfaces operating in a convective environment, Appl. Mech. Rev. 45 (5) (1992) 155–173.
[3] A. Bejan, Heat Transfer, Wiley, New York, 1993.
[4] A. Kraus, A. Snider, The choking and optimization of extended surface arrays, J. Heat Transfer 107 (1985) 746.
[5] A.D. Kraus, Developments in the analysis of Finned arrays, in: Donald Q. Kern Award Lecture, National Heat Transfer Conference, Baltimore, MD, August 11, 1997, Internat. J. Transport Phenomena 1 (1999) 141–164.
[6] A. Alebrahim, A. Bejan, Constructal trees of circular fins for conductive and convective heat transfer, Internat. J. Heat Mass Transfer 42 (1999) 3585–3597.
[7] A. Bejan, N. Dan, Constructal trees of convective fins, J. Heat Transfer 121 (1999) 675–682.
[8] A. Bejan, Shape and Structure from Engineering to Nature, Cambridge University Press, Cambridge, 2000.
[9] A. Bejan, S. Lorente, The constructal law and the thermodynamics of flow systems with configuration, Internat. J. Heat Mass Transfer 47 (2004) 3203–3214.